

NOTES AND CORRESPONDENCE

A Conservative Quasi-Monotone Semi-Lagrangian Scheme

RODOLFO BERMEJO

Departamento de Matemática Aplicada, Universidad Complutense de Madrid, Madrid, Spain

JUSTO CONDE

Instituto Nacional de Meteorología, Madrid, Spain

13 April 2000 and 12 June 2001

ABSTRACT

A conservative quasi-monotone semi-Lagrangian scheme is developed in this paper. Mass conservation is achieved via Lagrange multipliers. The new scheme is computationally efficient. Numerical examples with linear and nonlinear advection problems illustrate the properties of the scheme.

1. Introduction

We present in this paper a new conservative version of the quasi-monotone semi-Lagrangian (QMSL) scheme of Bermejo and Staniforth (1992). The idea of constructing the QMSL scheme was inspired by Zalesak's approach (Zalesak 1979) to improve the first flux-corrected transport scheme of Boris and Book (1973). Hereafter, whenever we refer to a numerical method as mass conservative, or simply conservative, we mean that is so with respect to $\int u \, dx$, where u is the exact solution of the problem at hand. It is recognized that mass conservation is a desirable property that numerical methods, which are used in long-term simulations such as climate studies and ocean circulation, should possess. Priestley (1993) developed an algorithm to endow conservation to the QMSL scheme of Bermejo and Staniforth. Although excellent results have been reported in the literature using Priestley's scheme (see, e.g., Gravel and Staniforth 1994; Priestley 1993), there are some pathological cases in which such an algorithm may not achieve conservation. The new conservative QMSL achieves global conservation via a variational formulation of the conservation property and, what is more interesting, is easy to implement. The layout of this note is as follows. In section 2, we describe the theoretical formulation of the new scheme, whereas section 3 is

devoted to illustrating its behavior with some numerical tests. The main conclusions are presented in section 4.

2. The conservative QMSL scheme

To make the presentation of the new scheme as simple as possible, let us consider the linear advection equation for a scalar $u(\mathbf{x}, t)$ in a bounded domain Ω with boundary Γ :

$$\begin{aligned} \frac{\partial u}{\partial t} + \mathbf{a} \cdot \nabla u &= 0, & \text{in } \Omega \times [0, T], \\ u(\mathbf{x}, 0) &= u_0(\mathbf{x}) & \text{in } \Omega, \end{aligned} \quad (1)$$

and appropriate boundary conditions such that

$$\int_{\Omega} u(\mathbf{x}, t) \, dx = \int_{\Omega} u_0(\mathbf{x}) \, dx, \quad (2)$$

whenever the velocity vector $\mathbf{a}(\mathbf{x}, t)$ is divergence free. We shall consider below the case when $\nabla \cdot \mathbf{a}(\mathbf{x}, t) \neq 0$. $[0, T]$ denotes the time interval for the integration of (1) and (2), and $u_0(\mathbf{x})$ is the initial condition for $u(\mathbf{x}, t)$. To compute a numerical solution of (1) and (2) the domain Ω is covered by a grid and the interval $[0, T]$ is substituted by the discrete set $\{t_n, 0 \leq n \leq N; t_0 = 0 \text{ and } t_N = T\}$. To make things simple, we assume that for all n , $\Delta t = t_n - t_{n-1}$ is the constant time step, and Ω is a two-dimensional rectangular domain that is covered by a uniform grid. We denote by h the distance between consecutive grid points in each coordinate direction. Let K be the number of grid points in Ω and

Corresponding author address: Rodolfo Bermejo, Facultad de CC. Matemáticas, Departamento de Matemática Aplicada, Universidad Complutense de Madrid, 28040 Madrid, Spain.
E-mail: rbermejo@amb-to.uclm.es

$\{\mathbf{x}_k\}$, where $k = 1, 2, \dots, K$, is the set of such grid points. Each \mathbf{x}_k can be identified by its coordinates as

$$\mathbf{x}_k \equiv (x_i, y_j) = [x_1 + (i - 1)h, y_1 + (j - 1)h],$$

where i and j are integers that satisfy $1 \leq i \leq I, 1 \leq j \leq J$, and $K = I \times J$. The pair (i, j) and the index k satisfy, for example, the relationship

$$k = (i - 1)J + j.$$

Hereafter, we use the notations u_k^n and U_k^n to denote the exact and approximate solutions of (1) and (2), respectively, at (\mathbf{x}_k, t_n) . For all k , the numerical semi-Lagrangian solution at (\mathbf{x}_k, t_{n+1}) is then

$$U_k^{n+1} = U^n(\mathbf{X}_k^n), \tag{3}$$

where \mathbf{X}_k^n denotes an approximate value of $\mathbf{X}(\mathbf{x}_k, t_{n+1}; t_n)$, which is the departure point at time t_n of a particle that moving with velocity \mathbf{a} will arrive at the grid point \mathbf{x}_k at t_{n+1} . Here, $\mathbf{X}(\mathbf{x}_k, t_{n+1}; t_n)$ is the solution of the differential equation,

$$\frac{d\mathbf{X}(\mathbf{x}_k, t_{n+1}, t_n)}{dt} = \mathbf{a}[\mathbf{X}(\mathbf{x}_k, t_{n+1}; t_n), t], \quad t_n \leq t \leq t_{n+1},$$

$$\mathbf{X}(\mathbf{x}_k, t_{n+1}; t_{n+1}) = \mathbf{x}_k, \tag{4}$$

under fairly mild assumptions about \mathbf{a} . In general, \mathbf{X}_k^n is not a grid point, so that $U^n(\mathbf{X}_k^n)$ has to be computed by some interpolation procedure from the known values U_j^n at grid points that surround \mathbf{X}_k^n . The most common interpolation procedure used in semi-Lagrangian methods is Lagrange polynomial interpolation of a degree higher than one, in particular cubic interpolation since it represents a good compromise between accuracy and computational efficiency. Other interpolation procedures such as cubic splines and cubic Hermite polynomials are also used. The solution obtained by any interpolation procedure is, in general, not conservative, and if its degree is higher than one, then the solution will exhibit strong oscillations in the vicinity of regions of rapid spatial variations. Bermejo and Staniforth (1992) invented the QMSL scheme to suppress such oscillations and restore to the numerical solution the positivity properties of the exact solution, but the QMSL scheme does not have the property of mass conservation. In this paper we provide mass conservation to the QMSL scheme through the following two stages.

a. The QMSL stage

This stage is essentially the QMSL scheme as is described in section 2 of Bermejo and Staniforth (1992). However, for completeness of this note we furnish a brief description of it, and refer the interested reader to that paper for further details. Let $\{U_{k_1}^n, U_{k_2}^n, \dots, U_{k_p}^n\}$ be the gridpoint values of U^n at the vertices of the grid element where the departure point \mathbf{X}_k^n is located, and let U_{Lk}^{n+1} and U_{Hk}^{n+1} be the values of a low-order solution and

a high-order solution at \mathbf{X}_k^n , respectively; U_{Lk}^{n+1} is obtained from U^n by Lagrange polynomial interpolation of degree one, which is known to be shape preserving, whereas U_{Hk}^{n+1} is calculated by an interpolation procedure of a degree higher than one, which, in general, is not shape preserving because it may exhibit an oscillatory behavior. The QMSL stage combines both solutions in a clever way to yield a nonoscillatory solution. As is shown in Bermejo and Staniforth (1992), the QMSL stage can be formulated as follows.

At each instant $t_{n+1}, n = 0, 1, \dots, N$, and for $k = 1, 2, \dots, K$, perform the following steps.

Step 1. Compute \mathbf{X}_k^n and identify the grid element where such a point is located.

Step 2. Calculate U_{Lk}^{n+1} and U_{Hk}^{n+1} as mentioned above.

Step 3. Evaluate U^+ and U^- defined as

$$\begin{cases} U^+ = \max\{U_{k_1}^n, U_{k_2}^n, \dots, U_{k_p}^n\} & \text{and} \\ U^- = \min\{U_{k_1}^n, U_{k_2}^n, \dots, U_{k_p}^n\}. \end{cases} \tag{5}$$

Step 4. Set

$$\begin{aligned} \bar{U}_k &= U^+ & \text{if } U_{Hk}^{n+1} > U^+, & \text{ or} \\ \bar{U}_k &= U^- & \text{if } U_{Hk}^{n+1} < U^-, & \text{ or} \\ \bar{U}_k &= U_{Hk}^{n+1} & \text{otherwise.} \end{aligned}$$

b. The conservation stage

The QMSL solution \bar{U} computed in the previous stage will not in general conserve mass, or equivalently, at each time step t_n

$$\sum_k \bar{U}_k S_k \neq C,$$

where C is a constant defined as

$$C = \sum_k u_{0k} S_k, \tag{6}$$

which is a numerical approximation to the initial mass $\int u_0 dx$. Here, S_k is the area associated with node k . In a uniform grid, $S_k = h^d$ for all k , with d being the dimension of the space. The case of a nonuniform grid is illustrated in Fig. 1. Inspired by a postprocessing procedure devised by Sasaki (1976), which has recently been used by Hansbo (2000) to conserve mass in adaptive finite elements, we create a method to restore the lost mass in the QMSL stage. Basically, this method consists of finding a new grid function $V = \{V_1, V_2, \dots, V_K\}$ such that a weighted mean square error between V and \bar{U} is minimum and $\sum_k V_k S_k = C$. Mathematically, this idea can be formulated as a constraint minimization problem as follows. Let U^n be the quasi-monotone and conservative solution ($C = \sum_k U_k^n S_k$) at instant t_n , and let \bar{U} be the QMSL solution (nonconservative) at instant t_{n+1} . The constrained minimization problem is as follows:

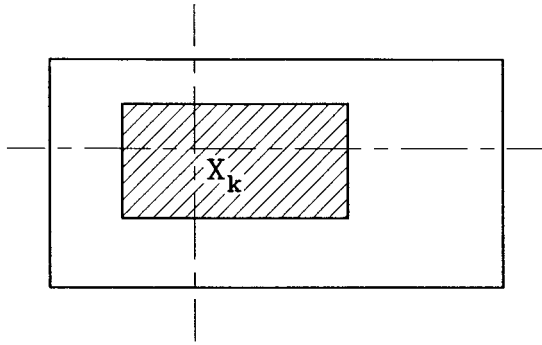


FIG. 1. The shaded area is the area S_k associated with grid point \mathbf{x}_k on a nonuniform grid.

At each instant t_n , $n = 1, 2, \dots, N$, find a grid function V such that

$$\begin{cases} \frac{1}{2} \sum_k \frac{(V_k - \bar{U}_k)^2}{w_k} S_k = \min! \\ \sum_k V_k S_k = \sum_k U_k^n S_k = C, \end{cases} \quad (7)$$

where w_k are gridpoint values of a nonnegative weight function w that is used in order to make V quasi-monotone too. Note that the first equation in (7) means that the grid function V is such that the weighted root-mean square of $V - \bar{U}$ is a minimum. Since (7) represents an optimization problem with constraints, then a practical method to find its solution is to formulate it as a saddle point problem by using the method of Lagrange multipliers. To do so, we define the function

$$F(V, \lambda) = \frac{1}{2} \sum_k \frac{(V_k - \bar{U}_k)^2}{w_k} S_k - \lambda \sum_k (V_k - U_k^n) S_k,$$

where the parameter λ is the Lagrange multiplier of the mass conservation constraint. Next, we wish to find V and λ such that the pair (V, λ) is a critical point of F . This is equivalent to finding (V, λ) from the equations

$$\frac{\partial F}{\partial V_k} = 0 \quad \text{for all } k, \quad \text{and} \quad \frac{\partial F}{\partial \lambda} = 0.$$

In so doing, one can easily obtain

$$V_k = \bar{U}_k - \lambda w_k \quad \text{for all } k, \quad \text{and} \quad (8)$$

$$\lambda = \frac{\sum_k (\bar{U}_k - U_k^n) S_k}{\sum_k w_k S_k} = \frac{\sum_k \bar{U}_k S_k - C}{\sum_k w_k S_k}. \quad (9)$$

Note that by virtue of (8) and (9), and as long as $w_k \neq 0$ for some k , the conservation of mass is fully achieved regardless the values of the weights w_k . To determine these values we further require V to be quasi-monotone as is \bar{U} . Note that in the process of making the quasi-monotone solution \bar{U} be conservative, the quasi-monotone property can be lost. So, to determine V we shall try to match in an optimal way requirements

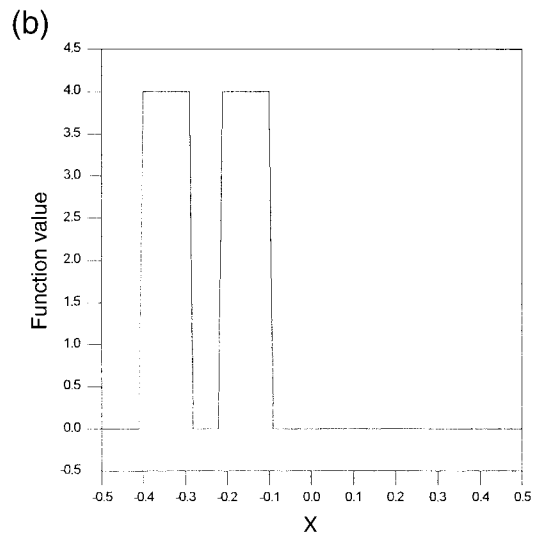
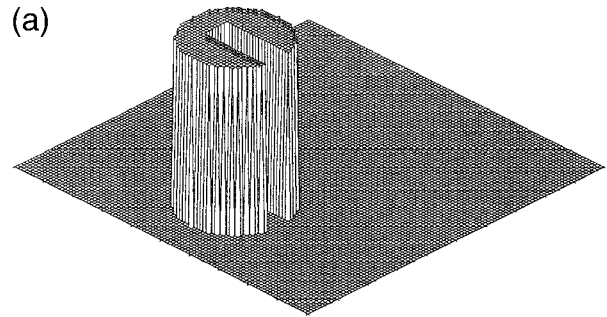


FIG. 2. (a) Slotted cylinder at $t = 0$. (b) Cross section of (a) at $y = 0$.

such as accuracy, conservation, and quasi-monotonicity. It is relatively easy to get accuracy and quasi-monotonicity as the QMSL stage does, see Bermejo (2001), but to calculate the grid function V possessing these three properties together is not straightforward, because they are somehow opposite. In order to match conservation and accuracy in V we consider (8) and use the property proved in Bermejo (2001), which says that in regions where the exact solution u is sufficiently smooth \bar{U} behaves as the high-order solution in such regions, that is, the numerical error is very small; whereas in those regions of low smoothness of u , the error $u - \bar{U}$ is large. Hence, we calculate the weights w_k in such a way that they are very small in the regions where u is sufficiently smooth, whereas in the regions where u is not smooth we allow w_k to be large. An expression for w_k satisfying these requirements might be $w_k = (U_{HK}^{n+1} - U_{LK}^{n+1})^p$, where p is an integer to be determined below. To match now the quasi-monotonicity ingredient with conservation and accuracy we recall (see Bermejo and Staniforth 1992) that the QMSL solution can also be expressed for all k and for all t_{n+1} , as $\bar{U}_k = U_{LK}^{n+1} +$

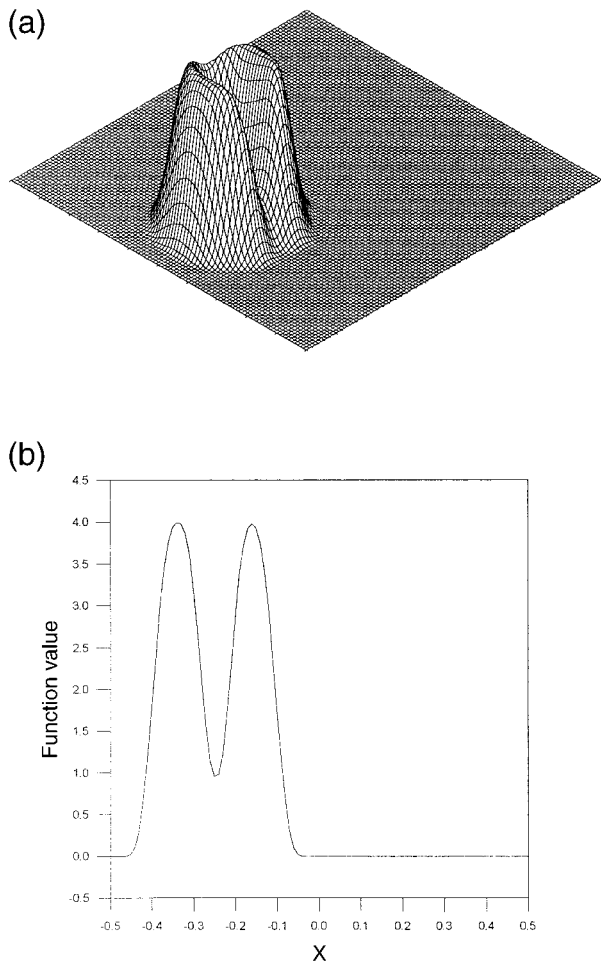


FIG. 3. (a) Slotted cylinder after six revolutions. (b) Cross section of (a) at $y = 0$.

$C_k(U_{Hk}^{n+1} - U_{Lk}^{n+1})$, where C_k is a limiting coefficient that satisfies $0 \leq C_k \leq 1$; then, in order to obtain a similar expression for V_k , we write (8) for all k and for all t_{n+1} , as

$$\begin{aligned}
 V_k &= U_{Lk}^{n+1} + C_k(U_{Hk}^{n+1} - U_{Lk}^{n+1}) - \lambda(U_{Hk}^{n+1} - U_{Lk}^{n+1})^p \\
 &= U_{Lk}^{n+1} + [C_k - \lambda(U_{Hk}^{n+1} - U_{Lk}^{n+1})^{p-1}](U_{Hk}^{n+1} - U_{Lk}^{n+1}),
 \end{aligned}
 \tag{10}$$

where p is an integer ≥ 1 . Note that in (10), $C_k - \lambda(U_{Hk}^{n+1} - U_{Lk}^{n+1})^{p-1}$ may be considered as a modified limiting coefficient at node k such that V is both quasi-monotone and conservative.

It remains to be determined whether p is an odd or even number. To determine this, we argue in the following manner. In (9), let

$$\Delta m = \sum_k \bar{U}_k S_k - C.$$

If $\Delta m < 0$ (loss of mass), then $\lambda < 0$, so that we propose restoring mass at those grid points where $U_{Hk}^{n+1} - U_{Lk}^{n+1} < 0$. On the contrary, if $\Delta m > 0$ (gain of

mass) implies that $\lambda > 0$, and we propose removing the excess of mass from those grid points where $U_{Hk}^{n+1} - U_{Lk}^{n+1} > 0$. Since by definition $w_k \geq 0$ for all k , then by considering (10) we see that a convenient way of restoring or removing mass according to the aforementioned argument is taking

$$w_k = \max[0, \text{sgn}(\Delta m)(U_{Hk}^{n+1} - U_{Lk}^{n+1})^p], \text{ for all } k. \tag{11}$$

Hence, p has to be odd and greater than 1. A good value for p is 3, because we want $\lambda(U_{Hk}^{n+1} - U_{Lk}^{n+1})^{p-1}$ to be a high-order perturbation to the limiting coefficient C_k . Since in Bermejo (2001) it is proved that (in regions where the solution is sufficiently smooth) $C_k = 1 - O(h^2)$ and $\max|U_{Hk}^{n+1} - U_{Lk}^{n+1}| = O(h^2)$, it follows that a convenient value is $p = 3$. In summary, the new conservative QMSL (CQMSL) scheme can be formulated as follows:

For $k = 1, 2, \dots, K$, S_k and u_{0k} are known.

Step 1. Compute at t_o

$$C = \sum_k (u_0)_k S_k.$$

For $n = 1, 2, \dots, N$ do the following.

Step 2. Apply the QMSL stage to compute \bar{U} , U_{Hk}^n , and U_{Lk}^n .

Step 3. Compute

$$\Delta m = \sum_k \bar{U}_k S_k - C.$$

If $\Delta m = 0$, then set $\lambda = 0$ and $w_k = 0$ for all $k = 1, 2, \dots, K$. Go to step 6.

Step 4. For $k = 1, 2, \dots, K$ calculate

$$w_k = \max[0, \text{sgn}(\Delta m)(U_{Hk}^n - U_{Lk}^n)^3].$$

Step 5. Compute

$$\lambda = \frac{\Delta m}{\sum_k w_k S_k}.$$

Step 6. For $k = 1, 2, \dots, K$ set

$$U_k^n = U_k - \lambda w_k.$$

If in step 4 $w_k = 0$ for all k , then set $\lambda = 0$ and go to step 6.

c. The CQMSL algorithm for advection equations written in conservation form

We now describe how to apply the CQMSL algorithm to the advection equations written in conservation form in which $\nabla \cdot \mathbf{a}$ is not necessarily zero. Thus, we consider the equation

$$\begin{aligned}
 \frac{\partial u}{\partial t} + \nabla \cdot (\mathbf{a}u) &= 0, \quad \text{in } \Omega \times [0, T], \\
 u(x, 0) &= u_0(x) \quad \text{in } \Omega,
 \end{aligned}
 \tag{12}$$

and appropriate boundary conditions such that $\int_{\Omega} \nabla \cdot (\mathbf{a}u) dx = \int_{\Gamma} \mathbf{n} \cdot \mathbf{a}u ds = 0$. Recalling that the Jacobian determinant $J(\mathbf{x}, s; t) = \det\{[\partial \mathbf{X}(\mathbf{x}, s; t)]/\partial \mathbf{x}\}$ satisfies the equation (see, e.g., Chorin and Marsden 1990; Raviart 1985)

$$\frac{dJ(\mathbf{x}, s; t)}{dt} = J \nabla \cdot \mathbf{a}[\mathbf{X}(\mathbf{x}, s; t)] \quad J(\mathbf{x}, s; s) = 1, \quad (13)$$

the solution of which is

$$J(\mathbf{x}, s; t) = \exp \left\{ \int_s^t \nabla \cdot \mathbf{a}[\mathbf{X}(\mathbf{x}, s; \tau)] d\tau \right\}, \quad (14)$$

then, it is easy to see that (12) becomes

$$\begin{aligned} \frac{DJu}{Dt} &= 0, \quad \text{in } \Omega \times [0, T], \\ u(x, 0) &= u_0(x) \quad \text{in } \Omega. \end{aligned} \quad (15)$$

Hence, if we take $s = t_{n+1}$ and $t = t_n$ in the above equations, it follows that the semi-Lagrangian solution to (15) is

$$U_k^{n+1} = J_k^n U^n(\mathbf{X}_k^n), \quad (16)$$

where $J_k^n \equiv J(\mathbf{x}_k, t_{n+1}; t_n)$ is obtained by approximating the integral of (14) by some quadrature rule, as for example the trapezoidal rule, which yields $J_k^n = \exp[-\Delta t \nabla \cdot \mathbf{a}^{n+(1/2)}(\mathbf{X}_k^{n+(1/2)})]$. Here, $\nabla \cdot \mathbf{a}^{n+(1/2)}(\mathbf{X}_k^{n+(1/2)})$ can be calculated by interpolation from the values of $\nabla \cdot \mathbf{a}^{n+(1/2)}$ at the grid points. If we compare (16) with (3), it is clear how we have to modify the CQMSL algorithm when it is applied to compute the numerical solution to (12). In fact, besides the computation of $\nabla \cdot \mathbf{a}$ at the grid points at each time step, we have to modify step 1 and step 2 of the QMSL algorithm in the following way.

Modified step 1. Compute \mathbf{X}_k^n and J_k^n , and identify the element where \mathbf{X}_k^n is located.

Modified step 2. Calculate $U_{Lk}^{n+1} = J_k^n U_L^n(\mathbf{X}_k^n)$ and $U_{Hk}^{n+1} = J_k^n U_H^n(\mathbf{X}_k^n)$, where $U_L^n(\mathbf{X}_k^n)$ and $U_H^n(\mathbf{X}_k^n)$ denote low- and high-order solutions, respectively, at \mathbf{X}_k^n .

The other steps in algorithm QMSL and algorithm CQMSL remain unchanged.

Some remarks are now in order. First, with these modifications, it is straightforward to apply the CQMSL algorithm to calculate a numerical solution of the continuity equation $D\rho/Dt + \rho \nabla \cdot \mathbf{a} = 0$, ρ being the fluid density, when the incompressibility assumption does not hold. So that, if q denotes a mixing ratio, one can apply the CQMSL algorithm to calculate q when the flow is not divergence free, by solving the equation $D\rho q/Dt + \rho q \nabla \cdot \mathbf{a} = 0$ plus the continuity equation. Moreover, if at $t = 0$, $q = K \equiv \text{constant}$, the mixing ratio q will remain constant all the time due to the following reasons: (i) by virtue of (16) and the equations for ρ and ρq we have that at $t = t_1$, $(\rho q)_k^1 \equiv \rho_k^1 q_k^1 = J_k^0 (\rho q)^0(X_k^0)$ and $\rho_k^1 = J_k^0 \rho(X_k^0)$, respectively, (ii) it is well known in interpolation theory that a constant function remains

unchanged by any interpolation procedure, so that $\rho_k^1 q_k^1 = J_k^0 (\rho q)^0(X_k^0) = J_k^0 \rho^0(X_k^0) K = \rho_k^1 K$, hence $q_k^1 = K$. This argument can be applied to the solution at the next time step $t = t_2$ to get $q_k^2 = K$ and so on for any time step t_n . Second, there are other approaches to construct conservative semi-Lagrangian schemes such as the one proposed by Rančić (1992), who, based on the piecewise parabolic method of Colella and Woodward (1984), devised a local conservative semi-Lagrangian scheme; that is, a semi-Lagrangian scheme in which the average value of the dependent variable U at time t_{n+1} in each cell of the fixed grid is equal to the average value of U at time t_n in the corresponding cell of the grid generated by the departure points. This implies that global conservation of the semi-Lagrangian solution is achieved via local conservation at the deformed grid. This strategy to get global conservation is different from the one proposed in this paper, where global conservation is imposed as a constraint on the grid values of the semi-Lagrangian solution. In nonlinear conservation laws in which the solution (weak solution) develops shocks, which, roughly speaking, are jump discontinuities that move with a given velocity satisfying the so-called Rankine–Hugoniot relation, and such that the solution is smooth on both sides of the discontinuity, global conservation is needed for the shocks to move with the right velocities (see LeVeque 1992, and references therein); so that only conservative schemes are able to locate the shocks properly. The additional property of such schemes of being also locally conservative may be a bonus as far as the accuracy of locating the shocks is concerned. Summarizing, we may say that for those conservation problems where it is feasible to use semi-Lagrangian schemes, the CQMSL algorithm will give the right position (within an approximation error) of the jump discontinuities.

3. Numerical tests

To illustrate the behavior of the CQMSL scheme we have run some of the tests of Bermejo and Staniforth (1992). We use cubic Lagrange interpolation for all the results shown in this note. The first test is the passive advection of the “slotted” cylinder in the domain $[-1/2, 1/2] \times [-1/2, 1/2]$ covered by a uniform grid of step $h = 0.01$. The initial condition is defined by the slotted cylinder of radius $15h$ and height 4 centered at $(-1/4, 0)$, and is depicted in Fig. 2. The width of the slot is $6h$ and its depth is $22h$. The velocity $\mathbf{a} = \boldsymbol{\omega}(-x, y)$, with $\boldsymbol{\omega} = 0.3636 \times 10^{-4} \text{ s}^{-1}$, and the time step $\Delta t = 1800s$. So that, it is necessary to perform 96 time steps to complete a revolution. To monitor the behavior of the numerical solution we compute the quantities $[\sum_k U_k^n S_k]/[\sum_k (u_0)_k S_k]$ and $[\sum_k (U_k^n)^2 S_k]/[\sum_k (u_0^2)_k S_k]$. These quantities measure the “mass” and “energy” conservation properties of a numerical scheme, respectively. As in Bermejo and Staniforth (1992) we also monitor the maximum and minimum of the numerical

TABLE 1. Slotted cylinder using CQMSL scheme with cubic Lagrange interpolation.

Time step (s)	$\int U$	$\int U^2$	Max (U)	Min (U)	E_{DISS}	E_{DISP}
96	1.000	0.81	4.0	0.0	0.10 (-1)	0.80 (-1)
192	1.000	0.77	4.0	0.0	0.15 (-1)	0.92 (-1)
288	1.000	0.75	4.0	0.0	0.19 (-1)	0.10
384	1.000	0.73	4.0	0.0	0.22 (-1)	0.11
576	1.000	0.70	4.0	0.0	0.28 (-1)	0.12

solution as well as the dissipation E_{DISS} and dispersion E_{DISP} errors. Note that $E_{DISS} + E_{DISP} = \sum_k (u_k^n - U_k^n)^2 S_k$, which is the discrete mean square error. Table 1 shows the results given by the CQMSL scheme. These results should be compared with those of Table 3 of Bermejo and Staniforth (1992). We note that the CQMSL scheme is conservative, quasi-monotone, and slightly more dissipative than the QMSL scheme. Figures 2 and 3 show the initial condition and the numerical solution after six revolutions. Again, we note the excellent results given by the CQMSL scheme. As a final comment for this test, we have computed the departure points by scheme

2 of Temperton and Staniforth (1987), instead of using the exact solution of (4).

Our second test is the inviscid Burgers equation:

$$\frac{\partial u}{\partial t} + u \left(\frac{\partial u}{\partial x} + \frac{\partial u}{\partial y} \right) = 0, \quad \text{in } [-2, 2] \times [-2, 2] \quad \text{and}$$

$$t > 0,$$

$$u_0(x, y) = \frac{1}{4} + \frac{1}{2} \sin \frac{\pi}{2} (x + y),$$

and periodic boundary conditions. (17)

It is well known that the analytical solution $u(x, y, t) = u_0(x - ut, y - ut)$ develops shocks at time $T^* = 2/\pi$. For $t > T^*$, the method of characteristics does not work, or equivalently, the conventional semi-Lagrangian schemes will produce incorrect solutions. However, matters can be improved if we use the CQMSL scheme, because monotonicity ensures convergence and conservation will guarantee a correct shock location (LeVeque 1992), so that the CQMSL solution converges to a weak solution of the conservation law. Nevertheless, an entropy condition is still needed to prove the convergence

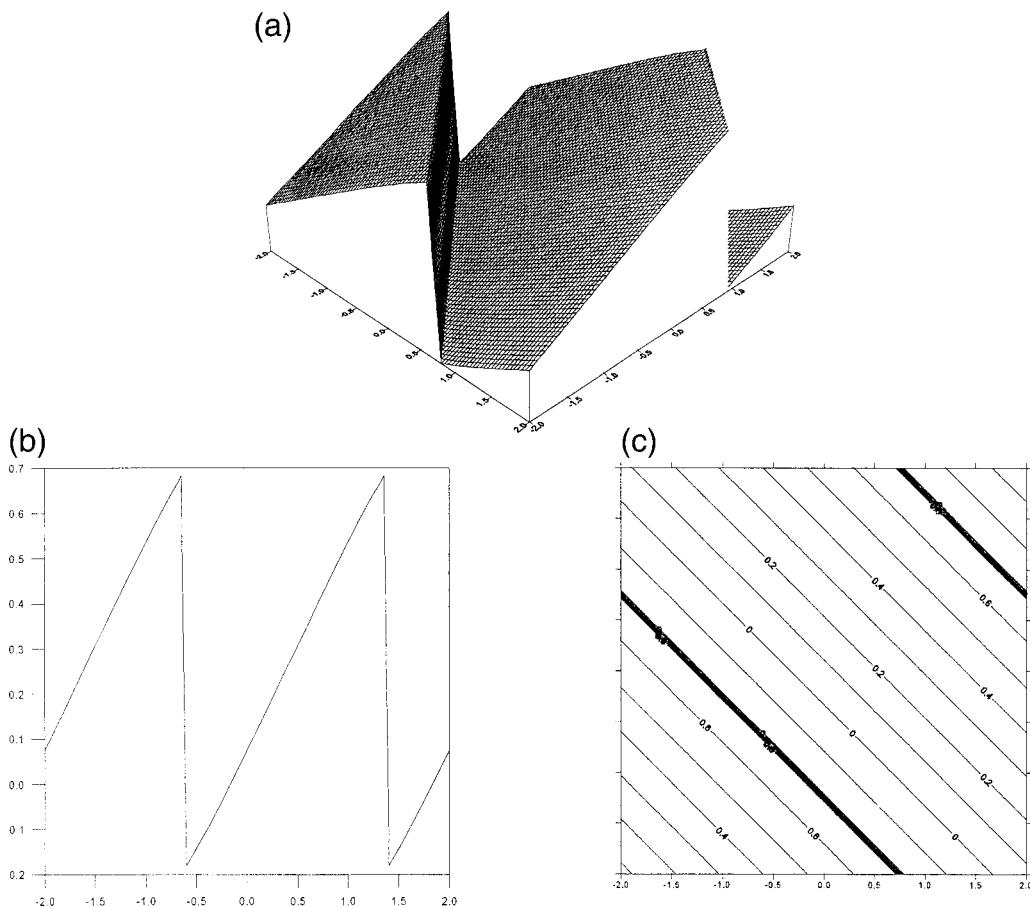


FIG. 4. A 2D CQMSL solution of the inviscid Burgers equation at $t = 1.5$ s. (a) Three-dimensional view. (b) A cross section along the main diagonal. (c) Level curves.

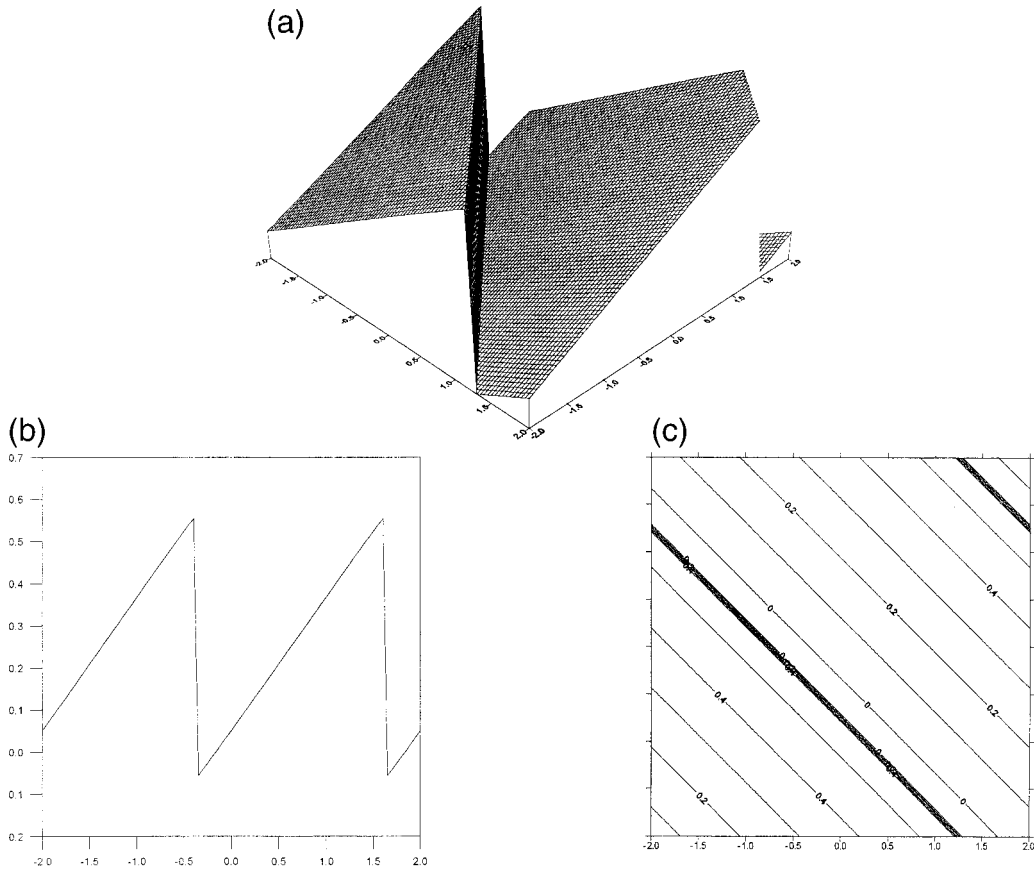


FIG. 5. A 2D CQMSL solution of the inviscid Burgers equation at $t = 2.5$ s. (a) Three-dimensional view. (b) A cross section along the main diagonal. (c) Level curves.

of the CQMSL solution to the correct weak solution of the problem, or in other words, to the correct physical one. At T^* the shocks start developing at the lines $x + y = \pm 2$. Some time after their development, the shocks interact with the expansion wave and this causes a rapid decay of the solution. In Figs. 4 and 5 we observe clearly the shocks located at the right positions and their displacement, as well as the decay of the solution with time. To obtain the results of these figures we have used $h = 0.0125$ and $\Delta t = 0.005$. A few remarks are now in order.

1) Observe that in (12) $u[(\partial u/\partial x) + (\partial u/\partial y)]$ can be written as $\mathbf{a}(u) \cdot \nabla u$, where $\mathbf{a}(u) = [a_1(u), a_2(u)]$, with $a_1(u) = a_2(u) = [\partial f(u)/\partial u]$, and $f(u) = (1/2)u^2$. Here, $\mathbf{a}(u)$ is the characteristic velocity and f is the flux function. The Rankine–Hugoniot condition (LeVeque 1992) establishes that if u_R and u_L denote the states to the right and left sides of the shock, then the shock velocity is given by the quotient

$$\frac{f(u_R) - f(u_L)}{u_R - u_L}.$$

So that, based on this condition, we approximate the velocity $\mathbf{a}(u)$ as

$$\begin{aligned} a_1(u)_k^n &= a_2(u)_k^n = \frac{\frac{1}{2}(u_{k+1}^n)^2 - \frac{1}{2}(u_{k-1}^n)^2}{u_{k+1}^n - u_{k-1}^n} \\ &= \frac{1}{2}(u_{k+1}^n + u_{k-1}^n). \end{aligned}$$

Since u is constant along the characteristics, we have determined the departure points simply by Euler’s method:

$$\mathbf{X}_k^n = \mathbf{x}_k - \mathbf{a}(u)_k^n \Delta t.$$

2) In linear problems, such as the slotted cylinder test, the Courant–Freidrichs–Lewy (CFL) number can take fairly large values and the numerical solution can still be very good. However, this may not be the case in nonlinear problems such as (17). For in this case, the numerical solution is good for CFL numbers ≤ 0.4 , whereas for the one-dimensional version of (17) excellent results (not shown in this paper) were obtained with CFL numbers larger than 1.0.

- 3) Based on our own limited experience, we hope that the CQMSL scheme improves the numerical solution obtained by conventional semi-Lagrangian schemes in atmospheric models as demonstrated by Gravel and Staniforth (1994) in their numerical results of the shallow water equations on the sphere.

4. Conclusions

We have introduced in this paper a conservative version of the QMSL scheme of Bermejo and Staniforth (1992). From a practical point of view there are a number of features that make the new CQMSL scheme very attractive. First, the CQMSL scheme can be incorporated into any semi-Lagrangian code very easily. Second, the new scheme is conservative, so that it could be very useful in long-term computations where loss (or gain) of conserved quantities is a relevant issue. Finally, the CQMSL scheme possesses excellent multidimensional shock-capturing properties, which makes the CQMSL scheme more widely applicable.

Acknowledgments. This research has been funded by Grant CLI98-1076 from Comisión Interministerial de Ciencia y Tecnología.

REFERENCES

- Bermejo, R., 2001: Analysis of a class of quasi-monotone and conservative semi-Lagrangian advection schemes. *Numer. Math.*, **87**, 597–623.
- , and A. Staniforth, 1992: The conversion of semi-Lagrangian advection schemes to quasi-monotone schemes. *Mon. Wea. Rev.*, **120**, 2622–2632.
- Boris, J. P., and D. L. Book, 1973: Flux corrected transport I, SHASTA, a fluid transport algorithm that works. *J. Comput. Phys.*, **11**, 38–69.
- Chorin, A. J., and J. E. Marsden, 1990: *A Mathematical Introduction to Fluid Mechanics*. Texts in Applied Mathematics, Vol. 4, Springer-Verlag, 168 pp.
- Colella, P., and P. R. Woodward, 1984: The piecewise parabolic method (PPM) for gas-dynamical simulations. *J. Comput. Phys.*, **54**, 174–205.
- Gravel, S., and A. Staniforth, 1994: A mass conserving semi-Lagrangian scheme for the shallow water equations. *Mon. Wea. Rev.*, **122**, 243–248.
- Hansbo, P., 2000: A free-Lagrange finite element method using space-time elements. *Comput. Methods Appl. Mech. Eng.*, **188**, 347–361.
- LeVeque, J. R., 1992: *Numerical Methods for Conservation Laws*. Lectures in Mathematics, ETH Zürich and Birkhäuser-Verlag, 214 pp.
- Priestley, A., 1993: A quasi-conservative version of the semi-Lagrangian advection scheme. *Mon. Wea. Rev.*, **121**, 621–629.
- Rančić, M., 1992: Semi-Lagrangian piecewise biparabolic scheme for two-dimensional horizontal advection of a passive scalar. *Mon. Wea. Rev.*, **120**, 1394–1406.
- Raviart, P. A., 1985: An analysis of particle methods. *Numerical Methods in Fluid Dynamics*, F. Brezzi, Ed., Lecture Notes in Mathematics, Vol. 1127, Springer-Verlag.
- Sasaki, Y. K., 1976: Variational design of finite difference schemes for initial value problems with an integral invariant. *J. Comput. Phys.*, **21**, 270–278.
- Temperton, C., and A. Staniforth, 1987: An efficient two-time-level semi-Lagrangian semi-implicit integration scheme. *Quart. J. Roy. Meteor. Soc.*, **113**, 1025–1039.
- Zalesak, S. T., 1979: Fully multidimensional flux corrected transport algorithms for fluids. *J. Comput. Phys.*, **31**, 335–362.